Chemical Physics Letters 819 (2023) 140450

Contents lists available at ScienceDirect

Chemical Physics Letters

journal homepage: www.elsevier.com/locate/cplett

Research paper

Interaction between acetylsalicylic acid and a cationic amphiphile model: An experimental approach using surface techniques

R. Flores-Sánchez [a], M. Bigorra-Mir [a], F. Gámez [b,*], T. Lopes-Costa [a], P.G. Argudo [c], M.T. Martín-Romero [c], L. Camacho [c], J.M. Pedrosa [a,*]

[a] Departmento de Sistemas Físicos, Químicos y Naturales, Universidad Pablo de Olavide, 41013 Seville, Spain
[b] Departamento de Química Física I, Universidad Complutense de Madrid, 28040, Madrid, Spain., 28040 Madrid, Spain
[c] Departamento de Química Física y Termodinámica Aplicada, Instituto Universitario de Nanoquímica IUNAN, Facultad de Ciencias, Universidad de Córdoba, Campus de Rabanales, Ed. Marie Curie, E-14071 Córdoba, Spain

HIGHLIGHTS

- The stability of ASA-ODA complexes is concentration-dependent.
- Beyond the solubility limit, the chromophore orientation changes upon compression.
- Aliphatic amines might be suitable candidates for molecular carriers.

GRAPHICAL ABSTRACT

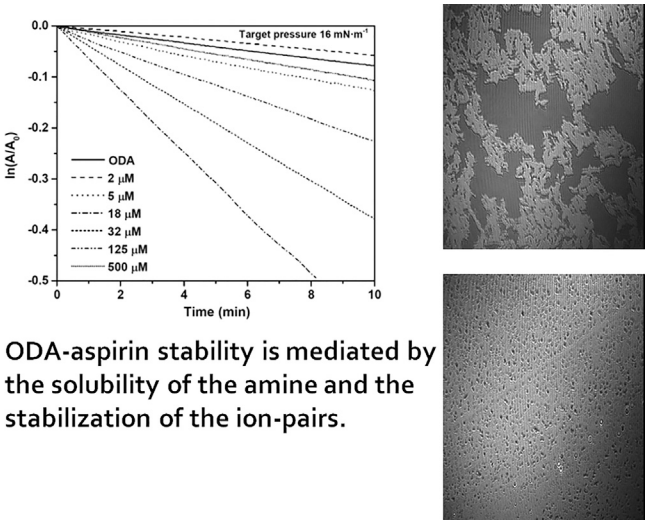

ARTICLE INFO

Keywords:
Drug–lipid interaction
Langmuir monolayer
Brewster angle microscopy
Reflection spectroscopy

ABSTRACT

Mechanical and morphological effects of monolayers of octadecylamine upon aspirin adsorption are monitored by Langmuir isotherms measurements and Brewster angle microscopy. Aspirin induced a notable expansion of the corresponding isotherms and a concentration-dependence of the mechanical stability of the films as a consequence of the subtle balance between the solubility of the amine and the monolayer stabilization induced by the ion-pairs, as corroborated by Brewster Angle Microscopy images. The incorporation of the aspirin into the interface was confirmed by UV–vis reflection spectroscopy. Some comments on the feasibility of using aliphatic amines for drug delivery of anionic species are presented.

* Corresponding authors.
E-mail addresses: frgamez@ucm.es (F. Gámez), jmpedpoy@upo.es (J.M. Pedrosa).

https://doi.org/10.1016/j.cplett.2023.140450
Received 9 January 2023; Received in revised form 10 March 2023; Accepted 20 March 2023
Available online 21 March 2023

1. Introduction

Changes in the rheological and mechanical properties of monolayers need to be understood at the molecular scale. Particularly, compression/deformation, collapse, the formation of three-dimensional clusters or the transference of matter to the subphase can be strongly influenced by the presence of molecules in the subphase, with dramatic effects in some cases [1]. Here, we will examine the effect of the subphase containing aspirin on monolayers of an aliphatic amine (octadecylamine, ODA). Although cationic lipids as those derived from the ethylphosphocholine (EPC) series might be more reliable for mimicking the interaction of aspirin within liposomes, ODA has been largely employed as a model of aliphatic amine able to generate an appropriate electrostatic environment required for the stabilization of Langmuir–Blodgett films of anionic species [2–6]. ODA has also been employed as part of molecular and nano-systems with different biomedical applications [7, 8]. Aspirin or acetylsalicilic acid (ASA) is widely used as a prophylactic agent for treating fever, cardiovascular diseases, pain and inflammation due to its inhibitory and non-selective effect on the cyclooxygenase [9] and it has been demonstrated that is a powerful drug for the prevention of some types of cancer [10] and neurodegenerative diseases [11,12]. In recent studios it has been observed that ASA engages strong interactions with mixed lipidic structures [13]. For these reasons, it is important to gain more fundamental information about the specific interaction of the drug molecule and anionic interfaces. Consequently, besides the fundamental knowledge, there exist an interest for studying this kind of interactions. Firstly, anionic lipids are of key importance in drug and gene delivery [14,15]. Moreover, the formation of (less toxic) anionic lipoplexes is mediated by a positively charged agent when handling with anionic drugs. Hence, the anionic drug/cationic amphiphile model constitutes a smart approach for the rational study of these systems, free from the presence of third intermediary reagents.

It is then justified that facing an experimental study dealing with the interaction of aspirin with cationic interfaces is more than convenient. In this work we have employed a plethora of surface techniques to accomplish this goal. Specifically, the ODA monolayer/aspirin system was characterized using surface pressure isotherms, Brewster angle microscopy (BAM) and UV–visible reflection absorption spectroscopy measurements. The main objectives were to identify how aspirin affects the molecular packing, morphology and stability from microscopic information. The possible incorporation of aspirin and related compounds in drug delivery systems is also discussed.

2. Materials and methods

2.1. Chemicals

Aspirin and ODA of reagent grade were supplied by Sigma Aldrich and have been used without further purification. Water was purified using a Millipore Direct-Q system (18 MΩ cm).

2.2. Instrumentation

Isotherms and hysteresis cycles were recorded in a computer-controlled NIMA 302LL Langmuir trough equipped with two removable Teflon barriers with a total area of 300 cm^2. The temperature was kept at 294 ± 0.5 K with a thermostat enclosure. The absence of surface-active contaminants was verified by compressing the bare water interphase and checking that the values of surface pressure were less than 0.1 mN m^{-1}. Monolayers were prepared by drop-wise spreading of an appropriate volume of chloroform solutions of ODA over the surface with a Hamilton microsyringe. After spreading, the solvent was allowed to evaporate for 15 min before measurement. The compression was started using two symmetrically moving barriers with a barrier speed set to 15 cm^2 min^{-1} (2.49 $Å^2$ per molecule per min for the experiments in MilliQ water). The surface pressure π is defined as $\pi = \gamma_0 - \gamma$ where γ_0 is the surface tension of the air/water interface and γ the surface tension in the presence of the amphiphilic. π was measured assuming a zero contact angle with a dynamometric sensor of Wilhelmy-type with a strip of Whatmans's Chr1 chromatography paper 10 mm wide. The reproducibility of the isotherms was tested by different measurements carried out in triplicate for independent samples.

Brewster Angle Microscopy (BAM) images were obtained with a I-Elli2000 (Accurion GmbH) with a lateral resolution of 2 μm coupled to a Nima 611D trough. The 532 nm *p*-polarized light coming from a diode laser is pointed towards the air–water interface at the water Brewster angle (53.15°). The image processing procedure included a geometrical correction of the image, as well as a filtering operation to reduce interference fringes and noise. The microscope and the film balance were located on a table with vibration isolation (antivibration system MOD-2 S, Accurion, Göttingen, Germany) in a large class 100 clean room.

Reflection spectroscopy measurements were performed with an Accurion RefSpec2 equipment with a spectral range of 220–1000 nm in a 702BAM Langmuir trough equipped with two Teflon barriers with a total area of 982 cm^2. A sensor unit collimates the light to the sample surface and focuses the reflected light into the optical fibers that guide it to the spectrometer. No polarizers were incorporated into the setup. A sample shutter is controlled via electronics holding a mirror that reflects the light directly to the detector fiber. It serves as a static reference to account for any lamp drift. The setup is completed with a blackplate located at the bottom of the Langmuir trough to eliminate stray light (absorbing and reflecting transmitted light out of the sensor). A single spectrum takes only less than 4 s to be performed. In each experiment, a number of reflection spectra were taken manually at different surface area values while the isotherms were being recorded. The selected area values were always the same in order to obtain results that could be comparable and reproducible. Series of spectra were taken in both compression and decompression cycles at surface areas ranging from 192 to 23 $Å^2$ per ODA molecule, obtaining 30 spectra per cycle.

3. Results

3.1. ODA-aspirin films spread on aspirin solutions

Our experiments were performed in a Langmuir trough by spreading chloroform solutions of ODA on pure water and on ASA aqueous solutions. Fig. 1 shows the corresponding isotherms of ODA on water and on ASA at different concentrations in the subphase. For ODA on water, the collapse surface pressure (~60 mN m^{-1}) and the limiting area (~20 $Å^2$ $molecule^{-1}$) are consistent with most values found in the literature [16–22]. There is a narrow molecular area range where gas-to-condensed phase transitions occurs before a small diminution of the molecular area leads to the collapse of the monolayers. As the ASA concentration increases, the corresponding isotherms undergo an expansion with shapes evolving to a continuous rising without apparent phase transitions, in contrast to typical saturated amphiphilic fatty acids (i.e., stearic acid, with the same chain length as ODA), where evident phase transitions take place under compression. We have measured additional isotherms keeping the macroscopic compression velocity (data not shown). We observed that when the ASA concentration is relatively low, a decrease in the microscopic velocity of compression lead to an increment of mass loss and a diminution of the surface pressure at a given molecular area, while at higher ASA concentrations, although the surface pressure also diminished with the decrease in the microscopic velocity, the mass transfer were significantly reduced but the shape of the isotherms are even more flat. Since this effect is a result of the balance between a kinetic process (solubilization of the monolayer) and thermodynamics (electrostatic stabilization), from now on all the experiments were performed at the same macroscopic velocity without loss of generality.

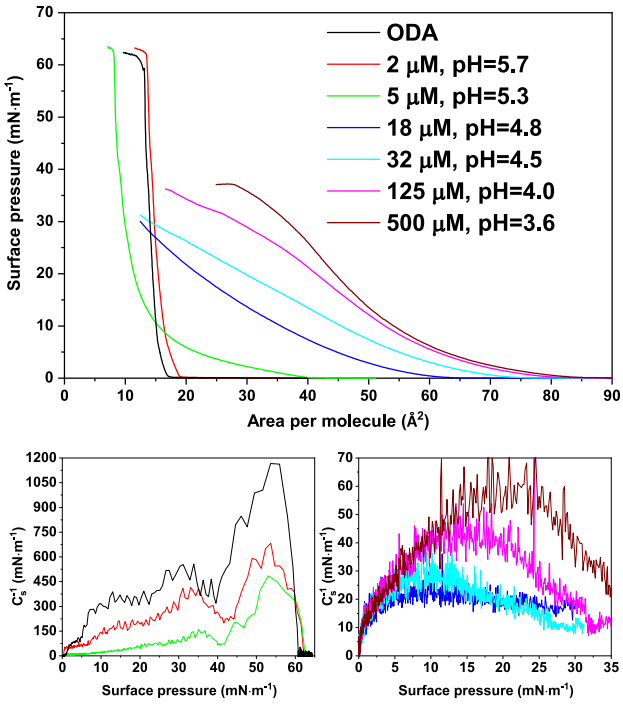

Fig. 1. (a) Surface pressure-area isotherms of ODA on ASA aqueous solutions. (b) Isothermal compressibility modulus as a function of the surface pressure. ASA concentrations are labeled in the graph.

Since pH conditions are below the bulk pK_a value of ODA (~10) and above that of ASA (~3.5), the major contribution to this interaction should be of coulombic type. In fact, the experimental pH values were found to be between 3.5 and 5.7, in very close agreement with the expected values from the dissociation of a weak acid with K_a~3 10^{-4}. The values are incorporated into the legend of Fig. 1. The interaction between anionic carboxylate groups of ASA and the cationic R–NH_3^+ moiety takes place when ASA^- ions approaches within the Debye volume yielding an electrostatic attachment. Hence, the expansion of the ODA monolayer when ASA is added to the subphase can be either due to a lateral coulombic and steric repulsion due to the incorporation of ASA^- into the films or by the modification of the electric double layer after the adsorption of these anions. It should be mentioned that, as the ionic strength of the aqueous subphase increases, the Debye length decreases and, as a consequence, the water H-bonds structure at the interface is disrupted [23,24]. This effect, together with the amphiphilic character of ASA [25] driven by its hydration Gibbs free energy [26], would be the main responsible phenomena for: (a) the enhanced incorporation of ASA into the ODA monolayer even at low ASA concentration, and (b) the prominent role played by electrostatic head-group–ASA interactions with respect to the tail-to-tail ones in such monolayers. These points will be treated in details by means of optical tools below.

Additionally, despite the adsorption of ASA on the ODA monolayer, the effect of the pH on the subphase also has an important effect on the shape and limiting molecular area extracted from the isotherms. These features have been reported by Albrecht et al. [27] They pointed out to the absence of measurable isotherms in the range $3<pH<5.6$ that was ascribed to an increment of the ODA solubility due to the sudden raise of hydrophilic interactions between headgroups [28]. Such behavior is less marked than expected due the collective behavior of surface charges that lowers the effective pK_a in the surface with respect to the bulk [29]. They also observed an incipient reappearance of more expanded isotherms at very low pH. Avazbaeva et al. and Sung et al. have studied this phenomenon using sum frequency generation, and hypothesized that the reappearance of the monolayer by lowering the pH down to ~2.5 is due to the charge screening of the remaining ODA ionizable sites by the (small) negative counterions [30,31]. Nevertheless, our experimental observations differ from those of ODA on water, since the introduction of an anion such as acetylsalicylate in the subphase leads to non-negligible surface pressure of ODA, notwithstanding the pH range enclosed that pH interval in which ODA should be strongly solubilized in water [30]. This fact might be due to the fact that ASA has a greater compensation effect, since is a larger cation than those used in those previous studies. Overall, in the present experiments there are two opposite effects that dominates in the different ASA concentration regimes as will be discussed in the next section. This first effect is the increasing solubility of ODA provoked by the increment of ionized sites as the pH diminishes, i.e., dissolution is proposed to be dominant in the range 0–5 μM. The second is the electrostatic and van der Waals interactions between ionized ODA moieties and ASA^- that tends to screen the effect of the enhanced solubility induced by the decrease of the pH, i.e., in the range 18–500 μM, electrostatics are proposed to be dominant. The stabilization of ODA films at low pH in the presence of large molecules is mentioned by Ganguly et al. [28] without further explanation. This balance will be better reflected in the study of the curves and stability of the monolayers described in the next subsection.

Information about the elasticity and a more sensitive analysis of phase transitions of the monolayers can be extracted from the slope of the isotherms by means of the real (elastic) part of the isothermal compressibility modulus $C_S^{-1} = -A\,(\partial\pi/\partial A)_T$. A larger compressibility modulus correlates with higher rigidity of the monolayer. The obtained values are shown in Fig. 1b. The compressibility modulus decreases as the monolayer approaches collapse. Together with the BAM imaged that will be discussed below, C_S^{-1} values indicate that ODA suffers a gas-to-solid transition or resublimation, while this transition is absent at sufficient ASA concentration. Increasing the ASA concentration has a notably influence on the monolayer that can be tracked by the lowering of the C_s^{-1} values with respect to water in the presence of ASA. This effect can be due to a destabilization of the more condensed phase due to a fluidization of the interface. These curves remains practically unchanged among the monolayers, irrespectively from the ASA concentration, and no collapse can be observed in the measurable π range. More details about the stability of the films will be provided in Section 3.2.

3.2. Dissolution dynamics and hysteresis curves

The dissolution dynamics of the films was studied by performing Langmuir trough experiments in which the molecular area is recorded as a function of time at a constant value of the surface pressure. The resulting isobars are plotted as A/A_0, where A is the specific area in a time t and A_0 the initial molecular area. The curves after an initial compression to 16 mN m^{-1} at the air-solution interface for the different ASA concentrations are shown in Fig. 2. This surface pressure corresponds to areas in which the ODA is entirely in the condensed phase (see Section 3.3 and Fig. 4) and ensure a measurable surface pressure of the monolayer spread on ASA during three subsequent compression/decompression cycles within the geometrical constraint of the experimental setup. The films experienced a significant area loss at the beginning of the experiment. As the bulk ASA concentration increases, the monolayer becomes more and more soluble in a progression dominated by the increasing solubility leading by the diminution of the pH. The only remarkably exception is the experiment performed for a concentration of 2 μM ASA. We believe that at this concentration, the decrease of the pH (enhancing the ODA dissolution) is still surpassed by the monolayer stabilization induced by the adsorption of ASA^-. At ASA concentrations higher than 18 μM, the tendency reverts because of the effect of the electrostatic and steric screening of ASA^- attached to or incorporated into the surface becomes dominant. Similar effects have been found for acidic compounds at the interface [32,33]. It is important to note that these experiments were performed for

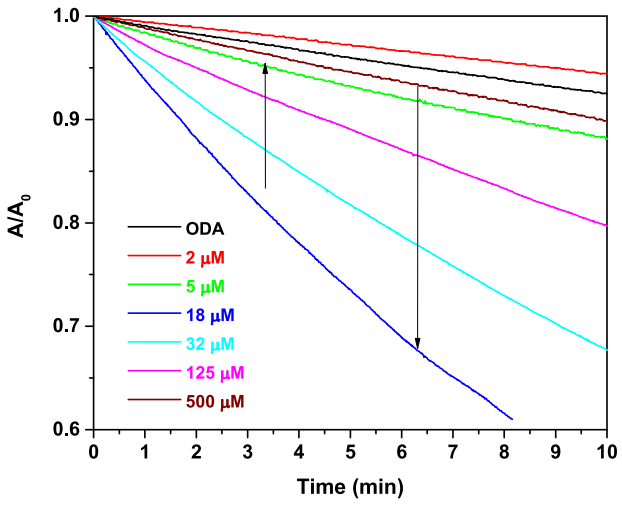

Fig. 2. Films stability of ODA films spreading at ASA aqueous solutions measured as the relative area (A/A_0, with A_0 the initial area) *vs* time curves at π=16 mN m^{-1}. The arrow indicates the stability trend.

more than 30 min for ODA and some of the low concentrated ASA cases. No asymptotic values were observed in any of the cases. For the less stable cases, the geometrical constraints of the trough precluded longer lasting measurements. All curves can be fitted to a first order solubility model of the form $\ln(A/A_0) \sim t$, indicating the importance of the solubility in the stability of the monolayers (see Figure S2 in the supporting information). It must be pointed out that the relaxation data in the literature – measured in the solubility-dominated pH region – are heterogeneous, probably because of the strong influence of waiting times and microscopic compression velocity in the initial packing state before the relaxation experiment starts [34,35].

The dissolution/stability of the monolayers has been further explored by means of hysteresis cycles. Hysteresis effects have been studied by means of three consecutive compression–expansion cycles for the ODA/ASA systems. The films were also compressed to a target pressure of 16 mN m^{-1} and subsequently decompressed until a negligible surface pressure was obtained. A differentiated behavior between the first compression and the consecutive decompression was observed for the different bulk concentrations of ASA. A closer inspection of the figure reveals several features. First of all, at low ASA concentration, a progressive diminution in the area values for the successive cycles accompanied by a general reduction in the corresponding hysteresis is observed. The first point is due to a loss of material toward the subphase during the compression process as discussed previously. However, no appreciable changes in the slope are observed among cycles, indicating that the rigidity of the films is retained in the process and hence no apparent conformational neither structural changes occur in the cycle-to-cycle sequence. Moreover, the non-coincidence of the second compression with the initial decompression curves can also be attributed to the fast dissolution process. The more intriguing effect is the different area changes between successive compression/decompression cycles of the isotherms with the ASA concentration. The higher degree of hysteresis (i.e., the difference between the area per molecule over successive compression/decompression cycles) is shown for the experiment with 18 μM of ASA in the subphase as shown in Fig. 3(h), where we have plotted the value of the variations of the specific area at 8 mN m^{-1} (one half the target pressure) in each cycle as a function of the ASA concentration in the bulk. Interestingly, this concentration is in accordance with the turning point observed in the dissolution dynamics experiments. From this concentration on, the successive hysteresis cycles inter-crossed and the degree of hysteresis diminishes again. This is likely a consequence of (i) the stabilization of the monolayer upon ASA$^-$ adsorption; and (b) the reorientational blocking provoked by the sudden changes in the interaction of ODA with water molecules in the presence of ASA$^-$ after the first compression. This supramolecular rearrangement after the first compression can also be the reason behind the crossing between the isotherms observed above. The increment of the film stability with the incorporation of an "amphiphilic" drug resembles the results of Mohammed et al. [36] and Fatouros and Antimisiaris [37]. Overall, these results reinforce the effects discussed in Section 3.1.

3.3. Brewster angle microscopy (BAM)

The morphology of the films at the mesoscopic scale was monitored by means of BAM. The obtained images for a set of ASA concentrations are shown in Fig. 4. The heading of the column indicates the ASA concentration and the labels in each image corresponds to the molecular areas and surface pressures states in which they are taken. In the ASA concentration range dominated by the electrostatic screening of acetylsalicylate (above 18 μM), homogeneous images are observed in agreement with the absence of phase transition observed in the isotherms for the surface pressure window considered in the experiments. Below these concentrations and in comparison with pure ODA, the morphology of the films show drastic morphological changes that we will describe in the following.

The structure of ODA domains is well known to possess bright condensed regions of dendritic-like morphology spread on a darker gas phase even at 0 mN m^{-1} that appears as a consequence of the higher interaction between the amine groups and water that ultimately leads to the coexistence of a very condensed phase with a gas phase [17,19]. According to the C_S^{-1} values obtained in Section A, the condensed phase shows solid features. These domains progressively cover the entire surface close to the lift-off point as the available area per molecule diminishes, while small portions of gas phase are still visible within the solid regions. Above the lift-off point, the homogeneity of the films becomes apparent and is characteristic of prototypical amphiphilic molecules in highly condensed states. At even higher pressures, there appeared some bright aggregates due to the beginning of the monolayer collapse *via* 3-dimensional clustering. The observed progression is consistent with the already explained phase transitions examined in the isotherms above. In the second column of that figure, the BAM images of ODA monolayers on ASA solution 2 μM is shown to present a similar morphology at high pressures, but the condensation is somehow precluded. At high molecular areas, the boundaries of the condensed (brighter) domains are more regular than those of pure ODA and these domains coexist with small and discotic domains that, upon compression, are fussed with the dendritic domains. When ASA concentration increases, the fractal-like domains disappear in favor of circular-shape domains. The compactness of these domains increases with the surface pressure until an homogeneous image appears. At ASA concentrations of 18 μM (third column of Fig. 4) one can recognize the formation of discotic domains which are bigger and looser than those observed in the previous experiments. At higher surface pressures these domains starts to cluster as can be checked by the appearance of bright dots. Similar effects are observed when a 32 μM ASA solution is used as a subphase. At even higher ASA concentration, the formation of solid clusters could not be detected within the experimental constraints due to the geometry of the Langmuir trough and all the images appears as homogeneous regions.

Within this scenario it becomes apparent that at the lowest ASA concentration, the lost of irregularity in the ODA domains are due to the enhance transference of molecules to the subphase. The rounded domains may correspond to ODA-rich domains which are effectively bounded to ASA anions, whose solubility is diminished due to the electrostatic screening provoked by the formation of the ion-pair. Hence, these types of morphology are dominant in the monolayer for higher

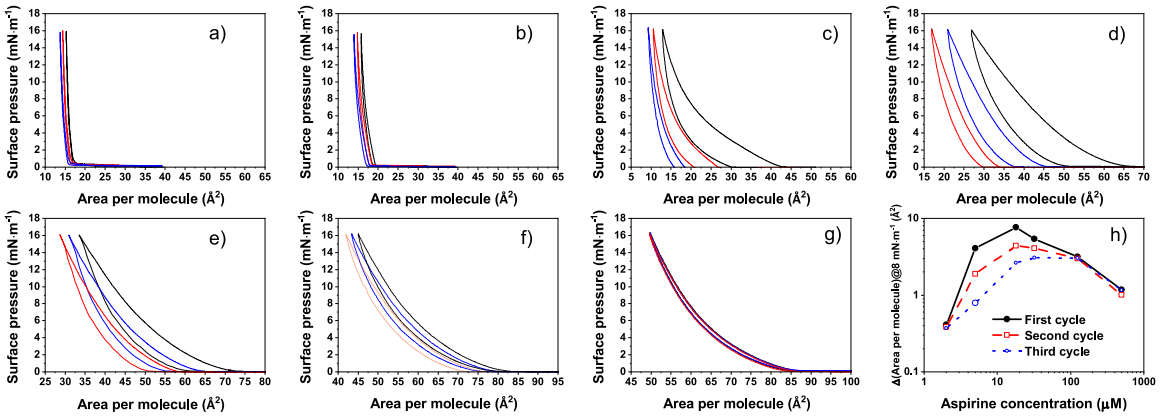

Fig. 3. Isotherms of three subsequent compression–expansion cycles of ODA monolayers on different ASA solutions at π=16 mN m^{-1}. Graphs are labeled in order of increasing ASA concentration: (a) 0 μM; (b) 2 μM; (c) 5 μM; (d) 18 μM; (e) 32 μM; (f) 125 μM (g) 500 μM. In panel h, the variations of the specific area at 8 mN m^{-1} in each cycle is presented.

ASA concentrations, but they tend to form homogeneous phases. In-between the cases of enhance-solubility and monolayer stabilization, one can still observed the formation of solid phases at high pressures in a sea of circular domains. These facts strengthen our previous outlined hypothesis of the differential behavior of the ODA monolayers in the presence of ASA in the subphase.

3.4. Reflection spectroscopy

In Fig. 5(a), the absorption in bulk solution of ASA and the reflection spectra of ODA monolayers on ASA subphases 0.5 mM is presented for different specific areas. This ASA concentration is chosen to bypass the relatively small molar extinction coefficient of ASA. The spectra of the monolayer have been normalized with the molecular area in order to cancel out the effect of the changes in the reflectivity provoked by the increment of the molecular density upon compression and, hence, the plotted parameter is the normalized reflection spectra ΔR_n. A clear indicative of the presence of aspirin at the interface is the reflection peak around 280 nm. This peak is characteristic of the adsorbed ASA molecules, since ODA has no optical activity in this wavelength region. Also, this evidence confirms the ability of ODA to retain this drug in the monolayer, as mentioned in the hysteresis studies. Furthermore, a small red-shift on the maximum absorption wavelength can be observed in the monolayer spectrum in comparison with the aqueous solution, shown as dashed lines in Fig. 5(a). This shift is likely be due to a change in the mesoscopic environment of ASA^- caused by interactions with the hydrocarbon chains of the ODA units, that ultimately lead to a less polar media. The diminution of the normalized reflection values upon compression can be due to:

(i) Given the size of the molecule, it is possible that the adsorbed ASA^- molecules leave the interface partially when compressed. To evaluate this latter case, further experiments have been done, and it has been demonstrated that with decompression the reflection peak is recovered as shown in Fig. 5(b). Therefore, in case this option is playing some role in the observed effect, it is a reversible process.

(ii) A loss of material towards the subphase. According to the hysteresis experiments, at this ASA concentration, and having into account the recuperation of the normalized spectra, the loss of materials can be ruled out.

(iii) The other possibility is that the molecule suffers a reorientation of the absorption transition dipole with respect to the incident electric field. This is possible because the molecule is large enough and could need a reorientation to remain attached to the ODA upon compression.

(iv) Finally, it should be noted that there is also an additional possibility that is related to the separation of the ASA^- ions from the amine groups that would be required for the accommodation to a tighter packing situation.

Assuming the reorientation as the most plausible explanation, a qualitative analysis is clear. As the surface pressure increases, the molecules evolve towards a more vertical position and the tilt angle of the transition dipole with respect to the electric field of the incident radiation progresses from 0 to higher values.

4. Conclusions

The interaction between membrane models and drugs is scarcely treated in the literature [38,39]. However, it is important to notice that the adsorption of aspirin to cationic lipids can play an important role in the development of a drug delivery system, being indispensable to obtain as much information at the molecular level as possible. Moreover, the relevance and utility of Langmuir monolayers at air/liquid interface as suitable models to study physical and chemical interactions at membranes surfaces has also been made evident. In this work, a set of experiments were conducted with the purpose of achieving a direct demonstration of the incorporation of the aspirin in ODA monolayers and its stability, using three important techniques: surface pressure isotherms, reflection spectroscopy and Brewster angle microscopy. The surface pressure-area isotherm of ODA reveals a large expansion with a disappearance of phase transitions as the bulk concentration of aspirin increases. The relaxation and hysteresis experiments indicate that the interaction between both molecules is modulated by the pH. Specifically, the subtle balance between the increasing ODA solubility in acidic media can be compensated by the electrostatic screening and steric hindrance of the acetylsalicylate anion that rise with the aspirin concentration. As a consequence, there is a maximum in ASA concentration for which the stability is minimum and the hysteresis degree is maximized. A further insight into this phenomenon is accomplished by a morphology study using Brewster angle microscopy proving the differential behavior of ODA monolayer with ASA concentrations. Finally, another important aspect that has been tested with the normalized reflection is the strength of the interaction and reorientation of the transition dipole that the molecule suffers in order to remain adhered to the monolayer. The results showed a reflection peak at 280 nm that correspond to the absorption of ASA, confirming not only the adsorption but the incorporation of aspirin to the lipid monolayer too. Given the mechanical properties previously described, we proposed a reorientation of the aromatic ring upon compression as the most probable explanation for the observed results. These experiments point to the possibility of using aliphatic amines as molecular carriers for anionic drugs or other biomedical applications, but the solubilization process must be reversed by (i) increasing the length of the aliphatic chain for obtaining an improve of the amphiphilic balance; or (ii) using the alkyl amines for the functionalization of biocompatible nanoparticles or by conjugation with other molecules [40,41].

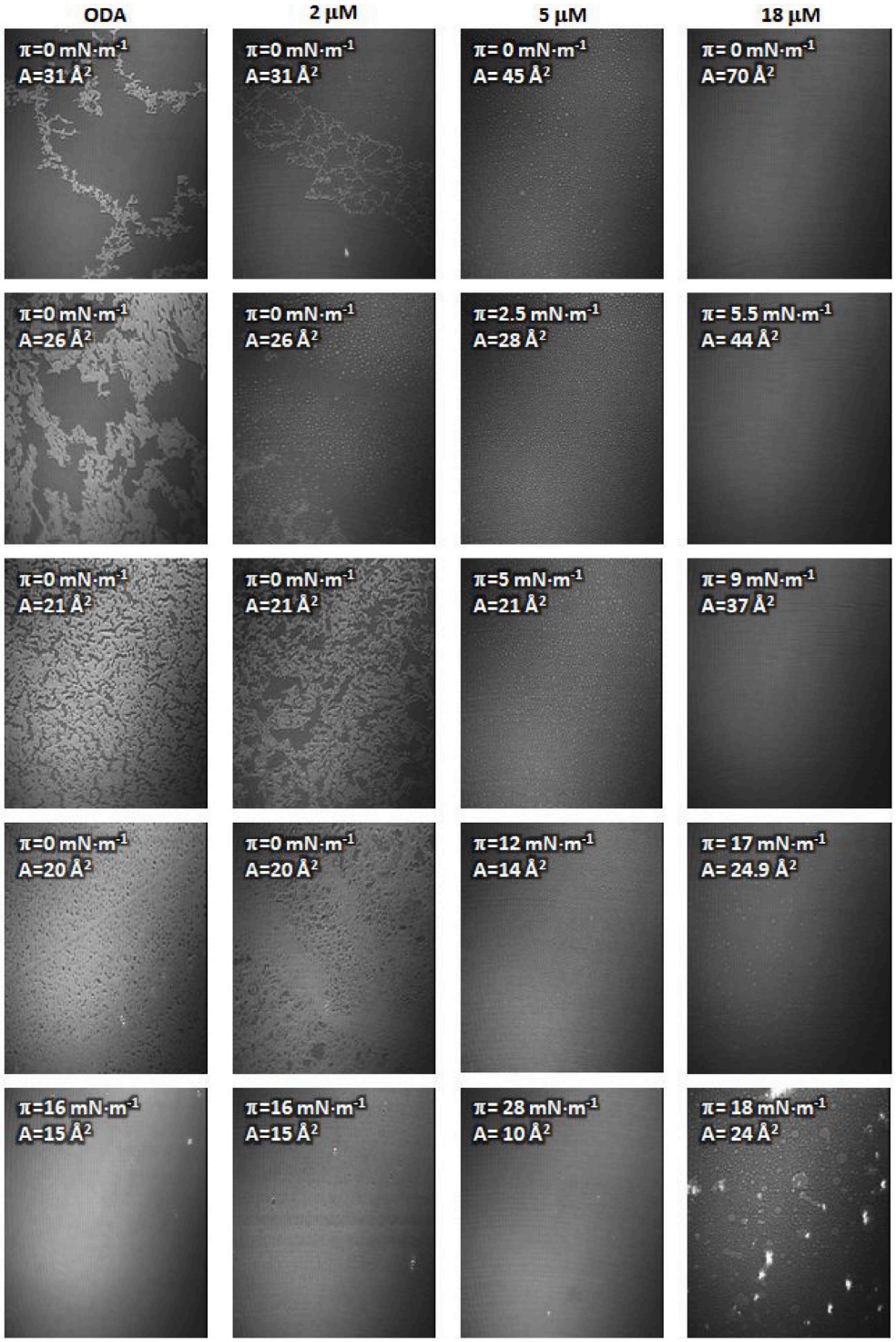

Fig. 4. Brewster Angle Microscopy images of ODA on ASA solutions at different concentrations under compression. First column corresponds to ODA on pure water subphase, the second one corresponds to ASA 2 μM, third column to 5 μM and the last one to 18 μM. The corresponding molecular areas and surface pressures are shown in the images. Image size: 430 μm width.

CRediT authorship contribution statement

R. Flores-Sánchez: Visualization, Investigation. **M. Bigorra-Mir:** Visualization, Investigation. **F. Gámez:** Conceptualization, Methodology, Original draft preparation, Writing – reviewing and editing. **T. Lopes-Costa:** Conceptualization, Methodology, Funding acquisition. **P.G. Argudo:** Visualization, Investigation. **M.T. Martín-Romero:** Conceptualization, Methodology. **L. Camacho:** Conceptualization, Methodology, Supervision, Resources. **J.M. Pedrosa:** Conceptualization, Methodology, Supervision, Resources, Writing – reviewing and editing, Funding acquisition.

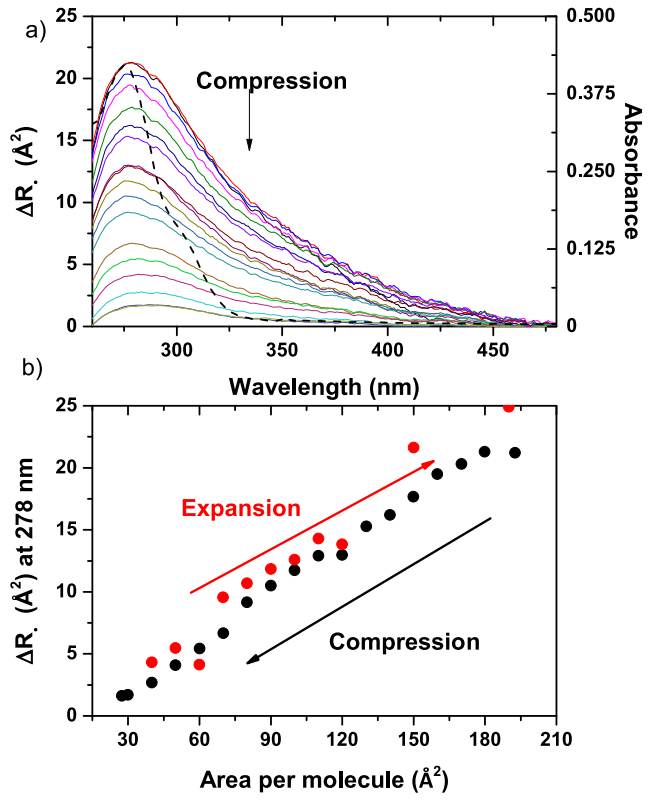

Fig. 5. (a) Normalized reflection spectra of ODA monolayers upon compression on 0.5 mM ASA subphase. The surfaces areas in which the spectra are taken are in the range 193–27 $Å^2$. The spectrum of ASA in solution is also included as a dashed line. (b) Values for the maximum of ΔR_n for a compression–decompression cycle.

Declaration of competing interest

The authors declare that they have no known competing financial interests or personal relationships that could have appeared to influence the work reported in this paper.

Data availability

Data will be made available on request

Acknowledgments

This work received financial support from the Ministry of Science and Innovation, the State Research Agency of Spain (AEI) (10.13039/501100011033, PID2019-105195RA-I) and the NextGenerationEU funds (PRTR), through projects PID2019-536 110430 GB-C22 (ADLIGHT) and PCI2020-112241 (SALMOS). The European Regional Development Fund and the Consejería de Transformación Económica, Industria, Conocimiento *y* Universidades de la Junta de Andalucía, in the framework of the Operative Programme FEDER-Andalucia 2014–2020 (objective 01) through projects P20_01258, P20_01234 and UPO-1381028 also contributed to the present research.

Appendix A. Supplementary data

Supplementary material related to this article can be found online at https://doi.org/10.1016/j.cplett.2023.140450.

References

[1] A. Ulman, An Introduction to Ultrathin Organic Films, first ed., Academic Press, New York, 1991.
[2] S. Gromelskim G. Bbrezesinski, DNA condensation and interaction with zwitterionic phospholipids mediated by divalent cations, Langmuir 22 (2006) 6293–6301.
[3] Y.L. Lee, Surface Characterization of octadecylamine films prepared by Langmuir–Blodgett and vacuum deposition methods by dynamic contact angle measurements, Langmuir 15 (1999) 1796–1801.
[4] V. Ramakrishnan, M. D'Costa, K.N. Ganesh, M. Sastry, Effect of salt on the hybridization of DNA by sequential immobilization of oligonucleotides at the air–water interface in the presence of ODA/DOTAP monolayers, J. Colloid Interface Sci. 276 (2004) 77–84.
[5] S. Erokhina, T. Berzina, L. Cristofolini, O. Konovalov, V. Erokhin, M.P. Fontana, Interaction of DNA oligomers with cationic lipidic monolayers: complexation and splitting, Langmuir 23 (2007) 4414–4420.
[6] M. Sastry, V. Ramakrishnan, M. Pattarkine, A. Gole, K.N. Ganesh, Hybridization of DNA by sequential immobilization of oligonucleotides at the air-water interface, Langmuir 16 (2007) 9142–9146.
[7] H. Yuan, J. Miao, Y. Du, J. You, F. Hu, S. Zeng, Cellular uptake of solid lipid nanoparticles and cytotoxicity of encapsulated paclitaxel in A549 cancer cells, Int. J. Pharm. 348 (1–2) (2008) 137–145.
[8] K. Debnath, K. Mandal, N.R. Jana, Phase transfer and surface functionalization of hydrophobic nanoparticle using amphiphilic poly(amino acid), Langmuir 32 (11) (2016) 2798–2807.
[9] M. Langecker, V. Arnaut, J. List, F.C. Simmel, DNA nanostructures interacting with lipid bilayer membranes, Acc. Chem. Res. 47 (6) (2014) 1807–1815.
[10] D.A. Drew, Y. Cao, A.T. Chan, Aspirin and colorectal cancer: the promise of precision chemoprevention, Nat. Rev. Cancer 16 (3) (2016) 173–186.
[11] S. Ayyadevara, M. Balasubramaniam, S. Kakraba, R. Alla, J.L. Mehta, R.J. Shmookler-Reis, Aspirin-mediated acetylation protects against multiple neurodegenerative pathologies by impeding protein aggregation, Antioxid Redox Signal 27 (17) (2017) 1383–1396.
[12] H. Chen, S. Zhang, M. Hernán, Nonsteroidal anti-inflammatory drugs and the risk of Parkinson disease, Arch. Neurol. 60 (2003) 1059–1064.
[13] R.J. Alsop, L. Toppozini, D. Marquardt, N. Kučerka, T.A. Harroun, M.C. Rheinstädter, Aspirin inhibits formation of cholesterol rafts in fluid lipid membranes, Biochim. Biophys. Acta 1848 (3) (2015) 805–812.
[14] B. Thapa, R. Narain, Mechanism, current challenges and new approaches for non viral gene delivery, in: R Narain (Ed.), Polymers and Nanomaterials for Gene Therapy, first ed., Elsevier, Cambridge, 2016, pp. 1–27.
[15] G. Vitiello, A. Luchini, G. D'Errico, R. Santamaria, A. Capuozzo, C. Irace, D. Montesarchio, L. Paduano, Cationic liposomes as efficient nanocarriers for the drug delivery of an anticancer cholesterol-based ruthenium complex, J. Mater. Chem. B 3 (2015) 3011–3023.
[16] Y.L. Lee, Surface characterization of octadecylamine films prepared by Langmuir–Blodgett and vacuum deposition methods by dynamic contact angle measurements, Langmuir 15 (1999) 1796–1801.
[17] Y.L. Lee, Y.C. Yang, Y.J. Shen, Monolayer characteristics of mixed octadecylamine and stearic acid at the air/water interface, J. Phys. Chem. B 109 (10) (2005) 4662–4667.
[18] S. Ye, H. Noda, T. Nishida, S. Morita, M. Osawa, Cd^{2+} induced interfacial structural changes of Langmuir–Blodgett films of stearic acid on solid substrates: a sum frequency generation study, Langmuir 20 (2004) 357–365.
[19] T. Lopes-Costa, F. Gámez, S. Lago, J.M. Pedrosa, Adsorption of DNA to octadecylamine monolayers at the air–water interface, J. Colloid Interface Sci. 354 (2011) 733–738.
[20] A. Mora-Boza, T. Lopes-Costa, F. Gámez, J.M. Pedrosa, Unveiling the interaction of DNA–octadecylamine at the air–water interface by ultraviolet–visible reflection spectroscopy, RSC Adv. 7 (2017) 5872–5879.
[21] P. Ganguly, D.V. Paranjape, F. Rondelez, Role of tail-tail interactions versus headgroup/subphase interactions in the pressure-area isotherms of fatty amines at the air-water interface. 1. Influence of subphase acid counterions, Langmuir 13 (1997) 5433–5439.
[22] S. Erokhina, T. Berzina, L. Cristofolini, O. Konovalov, V. Erokhin, M.P. Fontana, Interaction of DNA oligomers with cationic lipidic monolayers: complexation and splitting, Langmuir 23 (2007) 414–4420.
[23] X. Zhao, S. Ong, K.B. Eisenthal, New method for determination of surface pKa using second harmonic generation, Chem. Phys. Lett. 202 (1993) 513–520.
[24] D.E. Gragson, B.M. McCarty, G.L.J. Richmond, Ordering of interfacial water molecules at the charged air/water interface observed by vibrational sum frequency generation, J. Am. Chem. Soc. 119 (1997) 6144–6152.
[25] P. Dynarowicz, M. Paluch, B. Waligora, Surface orientation and effective dipole moments of some salicylic acid derivatives at the water/air interface, J. Colloid Interface Sci. 124 (2) (1998) 436–440.
[26] G.L. Perlovich, S.V. Kurkov, A.N. Kinchin, A. Bauer-Brandl, Solvation and hydration characteristics of ibuprofen and acetylsalicylic acid, AAPS J. 6 (2004) 22–30.

[27] O. Albrecht, H. Matsuda, K. Eguchi, Main and tilt transition in octadecylamine monolayer, Colloids Surf. A 284–285 (2006) 166–174.
[28] (a) P. Ganguly, D.V. Paranjape, F. Rondelez, Role of tail-tail interactions versus head-group-subphase interactions in pressure-area isotherms of fatty amines at the air–water interface. 1. Influence of subphase acid counterions, Langmuir 13 (1997) 5440–5446;
(b) P. Ganguly, D.V. Paranjape, K.R. Patil, Murali Sastry, F. Rondelez, role of tail-tail interactions versus head-group-subphase interactions in pressure-area isotherms of fatty amines at the air–water interface. 2. Time dependence, Langmuir 13 (1997) 5440–5446.
[29] E.S. Kartashynska, Y.B. Vysotsky, D. Vollhardt, V.B. Fainerman, Relationship between the bulk and surface basicity of aliphatic amines: a quantum chemical approach, ACS Omega 5 (49) (2020) 32032–32039.
[30] Z. Avazbaeva, W. Sung. J. Lee, M.D. Phan, K. Shin, D. Vaknin, D. Kim, Origin of the instability of octadecylamine Langmuir monolayer at low pH, Langmuir 31 (2015) 13753–13758.
[31] W. Sung, Z. Avazbaeva, D. Kim, Salt promotes protonation of amine groups at air/water interface, J. Phys. Chem. Lett. 8 (15) (2017) 3601–3606.
[32] L. Ghaicha, A.K. Chattopadhyay, H.A. Tajmirriahi, Behavior of stearic acid monolayers in presence of concentrated ammonium nitrate solution substrate, Langmuir 7 (10) (1991) 2007–2009.
[33] A.M. Brzozowska, M.H.G. Duits, F. Mugele, Stability of stearic acid monolayers on artificial sea water, Colloids Surf. A 407 (2010) 38–48.
[34] Y.-L. Lee, K.-L. Liu, Relaxation behaviors of monolayers of octadecylamine and stearic acid at the air/water interface, Langmuir 20 (2004) 3180–3187.
[35] Y.-L. Lee, Y.-C. Yang, Y.-J. Shen, Monolayer characteristics of mixed octadecylamine and stearic acid at the air/water interface, J. Phys. Chem. B 109 (2005) 4662–4667.
[36] A.R. Mohammed, N. Weston, A.G.A. Coombes, M. Fitzgerald, Y. Perrie, Liposome formulation of poorly water soluble drugs: optimisation of drug loading and ESEM analysis of stability, Int. J. Pharm. 285 (1–2) (2004) 23–24.
[37] D.G. Fatouros, S.G. Antimisiaris, Effect of amphiphilic drugs on the stability and zeta-potential of their liposome formulations: a study with prednisolone, diazepam, and griseofulvin, J. Colloid Interface Sci. 251 (2) (2002) 271–277.
[38] V.P.N. Geraldo, F.J. Pavinatto, T.M. Nobre, L. Caseli, O.N. Oliveira Jr., Langmuir films containing ibuprofen and phospholipids, Chem. Phys. Lett. 559 (2013) 99–106.
[39] E. Jabłonowska, R. Bilewicz, Interactions of ibuprofen with langmuir monolayers of membrane lipids, Thin Solid Films 515 (7–8) (2007) 3962–3966.
[40] Y. Yu, X. Yang, M. Liu, M. Nishikawa, T. Tei, E. Miyako, Anticancer drug delivery to cancer cells using alkyl amine-functionalized nanodiamond supraparticles, Nanoscale Adv. 1 (2019) 3406–3412.
[41] L. Qiu, M. Zhu, Y. Huang, K. Gonga, J. Chen, Mechanisms of cellular uptake with hyaluronic acid—octadecylamine micelles as drug delivery nanocarriers, RSC Adv. 6 (2016) 39896–39902.